A DSO-Driven Privacy-Preserving Mechanism for Managing Power Exchanges in Australian Networks

Seyed Amir Mansouri, Andrés Ramos, José Pablo Chaves Ávila, Javier García-González, and José A. Aguado, *Member, IEEE*

***Abstract*—This article presents a four-level hierarchical model to incorporate decentralized energy communities (ECs) into local electricity markets. The model utilizes an innovative distribution system operator (DSO)-driven algorithm to maximize grid services from ECs, monetize their energy surplus, and adapt market exchanges to network security constraints. In level 1, EC members determine their internal scheduling and power exchanges. A decentralized peer-to-peer (P2P) structure embedded in level 1 enables power sharing with dynamic pricing and limited data sharing among EC members. Levels 2 and 3 involve the EC operators and the retailer company determining their market strategies. In level 4, a DSO-driven algorithm is deployed to evaluate security constraints and the feasibility of exchanges between market players. Implemented on a modified 594-node distribution network in Victoria, Australia, the model optimally integrates ECs with local electricity markets. By preserving agents' privacy and keeping exchange details confidential, the proposed model ensures next-day contracts adhere to network security restrictions, maximizes grid services from ECs, and reduces members' electricity bills by 7.5%.**

***Index Terms*—Decentralized optimization, electric vehicles (EVs), energy community (EC), peer-to-peer (P2P) power sharing, smart grids.**

Received 27 November 2024; revised 26 February 2025, 22 March 2025, and 3 May 2025; accepted 27 June 2025. This work was supported in part by the Strategic Projects Program under Grant TED2021-131365B-C43, and in part by the NextGenerationEU/PRTR via the Spanish Ministry of Science and Innovation/State Research Agency. Paper no. TII-24-6347. *(Corresponding author: Seyed Amir Mansouri.)*

Seyed Amir Mansouri is with the Department of Engineering Systems & Services, Faculty of Technology, Policy & Management, Delft University of Technology, 2628 Delft, The Netherlands, also with the Institute for Research in Technology (IIT), ICAI School of Engineering, Comillas Pontifical University, 28015 Madrid, Spain (e-mail: s.mansouri@tudelft.nl).

Andrés Ramos, José Pablo Chaves Ávila, and Javier García-González are with the Institute for Research in Technology (IIT), ICAI School of Engineering, Comillas Pontifical University, 28015 Madrid, Spain (e-mail: aramos@comillas.edu; jchaves@comillas.edu; javierg@comillas.edu).

José A. Aguado is with the Department of Electrical Engineering, Escuela de Ingenierías Industriales, University of Malaga, 29010 Malaga, Spain (e-mail: jaguado@uma.es).

Digital Object Identifier 10.1109/TII.2025.3586048

NOMENCLATURE

Sets

c / ev	Set of EC operators/electric vehicles.
h,k	Sets of EC members.
i,j	Sets of network nodes.
sp / wt	Set of solar panels / wind turbines.
t / s / l	Set of times / scenarios / network lines.
Θ_c^h	Mapping set of members connected to ECs.
Θ_i^l	Mapping set of lines connected to nodes.
$\Theta_i^{sp/wt}$	Mapping set of DERs connected to nodes.

Parameters

$\gamma_{h\in\Theta_c^h,t}^{\text{Buy,ECO}\to\text{ECM}}$	Limit on power purchase from EC operators (%).
$\gamma_{h\in\Theta_c^h,t}^{\text{Sell,ECO}\to\text{ECM}}$	Limit on power sale to EC operators (%).
$\gamma_{i,t}^{\text{Limit,Buy/Sell}}$	Limit on nodal exchange for retailer (%).
π^{Imb}	Imbalance penalty ($/kWh).
$\pi_{k,t}^{P2P}$	P2P price ($/kWh).
π_{sp}^{SP}	Price of power from solar panels ($/kWh).
π_t^{MMR}	MMR price ($/kWh).
$\pi_t^{Op,\text{Buy/Sell}}$	Exchange prices with EC operators ($/kWh).
$\pi_t^{Ret,\text{Buy/Sell}}$	Exchange prices with retailer ($/kWh).
$\pi_t^{WSM,\text{Buy/Sell}}$	Exchange prices with WSM ($/kWh).
π_{wt}^{WT}	Price of power from wind turbines ($/kWh).
$\tau_{l,i}$	Power flow direction indicator.
$P_{h,t}^{Op-\text{Buy,max}}$	Max. Power purchase from EC operator (kW).
$P_{h,t}^{\text{Op}-\text{Sell,max}}$	Max. Power sale to EC operator (kW).
$P_{h,t}^{\text{Ret}-\text{Buy,max}}$	Max. Power purchase limit from retailer (kW).
$P_h^{\max}$	Capacity of member's metering system (kW).
$P_{i,t}^{\text{Fixed,Load}}$	Fixed loads (kW).
$P_t^{\text{Loss,T}}$	Sum of power losses per hour (kW).
PF_i	Reactive-to-active power ratio (%).
$S_l^{\text{Line,max}}$	Line capacity (kVA).
$P^{\text{Ret,min}}$	Min. power exchange limit with retailer (kW).

$P^{WSM,\max}$ Max. power exchange limit with WSM (kW).
$Rl/Bl/Gl$ Resistance/Susceptance/Conductance of line (p.u.).

Variables

$i_t^{WSM,\text{Buy/Sell}}$ Binary variables for power exchange with WSM.
$p_{h,t}^{\text{Op,Buy/Sell}}$ Power exchanges with EC operator (kW).
$p_{h,t}^{\text{Ret,Buy/Sell}}$ Power exchanges with retailer (kW).
$p_t^{WSM,\text{Buy/Sell}}$ Power exchange with WSM (kW).
$p_{h,t}^{\text{Net,Con}}$ Summation of power consumption per hour (kW).
$p_{h,t}^{\text{Net,Gen}}$ Summation of power generation per hour (kW).
$p_{h,t}^{P2P,\text{Available}}$ Available power per contract (kW).

I. Introduction

A. Background and Literature Review

MODERN energy communities (ECs) mark a shift in how energy is generated, consumed, and managed locally. Comprising smart households, businesses, and other stakeholders, ECs aim for self-sufficiency using distributed energy resources (DERs), such as solar panels, wind turbines, and battery storage. ECs can support grid stability by providing services, such as congestion management, frequency regulation, and voltage control. These services help balance supply and demand, integrate intermittent renewable energy sources (RESs), and enhance resilience. Active EC participation also enables more flexible grid operations, lowers infrastructure costs, and creates new revenue opportunities for members.

Several studies, including [1] and [2], have explored the technical and economic advantages of advanced technologies, such as peer-2-peer (P2P) power sharing, vehicle-to-home (V2H) systems, and thermostatically-controlled loads (TCLs) for members of ECs. These technologies enable more efficient energy use and cost savings by allowing EC members to share resources and manage their energy consumption dynamically. Research in [3] and [4] demonstrates that equipping EC members with these technologies can significantly reduce daily costs while enhancing their ability to provide grid services, thus contributing to overall grid stability and efficiency. Specifically, [1] and [2] focus on using the P2P platform for power sharing within ECs, facilitating local energy exchanges and promoting community resilience. In contrast, studies, such as [5], [6], [7], [8], and [9] investigate P2P power sharing between neighboring ECs, which can further optimize energy distribution and reduce reliance on external grid resources.

Many studies use distributed optimization to coordinate decentralized agents in local electricity markets. For instance, [2] and [7] utilize the alternating direction method of multipliers (ADMM) algorithm; Migoni et al.[10] employ tree-based model predictive control; Sivianes et al.[11] apply an accelerated distributed augmented Lagrangian method; Faraji et al.[12] and Zhao et al. [8] adopt game theory methods; Hong et al.[13] use a novel distributed event-triggered consensus control; Hui et al.[14] introduce a new distributed control scheme for coordinating market agents. While these methodologies offer optimal solutions and ensure agents' privacy, they often require considerable time for convergence and market settlement. In contrast, studies, such as [1], [3], [4], and [15], use centralized optimization for market agent coordination. This approach achieves rapid convergence but compromises privacy by necessitating the sharing of all agents' information with a centralized entity. Alternatively, works, such as , [5], [6], [9], [14], [16], [17], [18], and [19] employ hierarchical optimization techniques. These methods offer fast convergence and enhanced privacy protection for agents, although they may lead to slight deviations from the global optimal solution.

TABLE I
EVALUATION OF THE PROPOSED MODEL VERSUS RECENT STUDIES

Paper's information		EC members	EC operators	Retailer	Network Security Constraints		
Participation	Energy market	[1], [15], [10] [2], [11], [16] [12], [8], [18] [19], [3] [4], *	[15], [2], [11] [5], [6], [12] [7], [18] [19], [3] [4], *	[10] [8] [9] [3] [4], *	[1], [2], [6], [7], [9], [14] [19], *		
	Grid services	[2], [20], [13] [17], [18] [19], [21], *	[2], [18] [19], [21], *	[20] [13], *			
Market optimization	Centralized	[1], [15], [3], [4]			Technologies of End-Users	TCLs	[20], [13], [14] [17], [18], [21], *
	Distributed	[10], [2], [11], [12], [7], [8], [20], [13]				V2H	[10], [11], [8] [9], [3], *
	Hierarchical	[16], [5], [6], [9], [14], [17], [18] [19], *				P2P	[1], [2], [5], [6] [7], [8], [9] [3], [4], *

B. Research Gaps and Contributions

Table I compares the proposed model with recent studies, with an asterisk (∗) indicating the considered aspects. This table reveals a notable gap in the literature: While hierarchical optimization is well-documented for market applications, there is a lack of hierarchical structures that simultaneously include EC operators, EC members, retailers, and distribution system operator (DSOs) as independent decision-making agents in local electricity markets, each with their individual objectives and interests. Most studies either model EC members as aggregated loads controlled by EC operators, ignoring individual roles, or focus solely on EC members, neglecting EC operators. Few works [2], [18], [19] model both EC members and operators as decision-making actors for grid services, but none incorporate retailers or a full range of advanced technologies including P2P platform, battery-integrated solar (BIS), TCLs, and V2H systems. This gap limits understanding of how EC members can simultaneously manage P2P interactions, engage with EC operators and retailers, and optimize advanced technologies to generate revenue through grid services for DSOs.

To address the identified gaps, this article proposes a hierarchical model for integrating ECs into local electricity markets. The model incorporates EC members, EC operators, the retailer, and the DSO as independent agents, each optimizing its own schedule, while accounting for market signals and network constraints. It ensures secure integration with minimal data

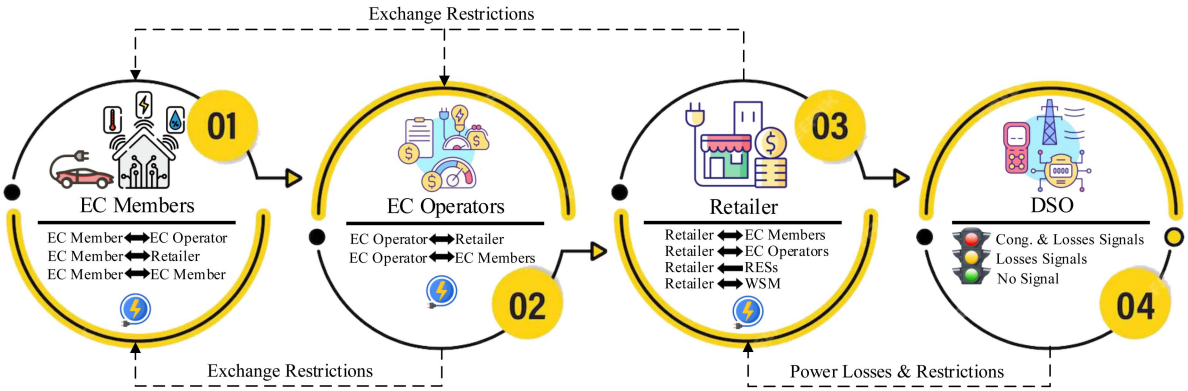

Fig. 1. Architecture of the proposed four-level hierarchical model.

sharing, activating EC flexibility for market participation and grid support. The key contributions are as follows.

1) Presenting a P2P-enabled hierarchical structure for local electricity markets, integrating EC members, EC operators, retailers, and DSOs into a four-level framework. It addresses local energy market and congestion issues, unlocking EC potential for grid services. This structure ensures high convergence speed and market settlement with limited data sharing, allowing agents to maximize interests while complying with network security.
2) Designing a decentralized P2P-enabled system for EC members' day-ahead scheduling. This setup allows EC members to meet their market needs via the P2P platform before engaging with upstream agents, such as EC operators and retailers. An enhanced Mid-Market Rate (MMR) method is introduced for dynamic pricing on the P2P platform, making exchanges more affordable for both buyers and sellers compared to those with upstream agents. This creates a competitive environment while reduces members' bills.
3) Presenting an innovative DSO-driven algorithm to ensure network security and maximize grid services from ECs. This algorithm enables the DSO to assess the feasibility of nodal exchanges without knowing their details, maintaining operational stability and market privacy. It enables the DSO to communicate security constraint violations and the required grid services through signals to market agents, prompting them to reschedule their initial exchanges accordingly. This ensures that finalized contracts adhere to network security constraints.

II. Model Outline

This article proposes a P2P-enabled hierarchical model that concurrently settles the local day-ahead energy market and mitigates congestion. As shown in Fig. 1, the model consists of four levels: 1) smart homes as EC members, 2) EC operators, 3) a retailer, and 4) the DSO. EC members and operators contribute to grid services by managing the flexibility of their loads. The hierarchical structure ensures minimal information sharing, limiting exchanges to traded power quantities. Market participants follow predefined hourly tariffs, while P2P prices are dynamically set by sellers. Each level is detailed as follows.

1) *First Level:* At this level, a decentralized P2P-enabled structure is presented for EC members' day-ahead scheduling. Each member can exchange power bidirectionally with other members, the EC operator, and the retailer. Transactions between members within the same community occur directly through the P2P platform, without intermediaries, and with a dynamic pricing mechanism. Each EC member, equipped with a BIS, an air conditioning (AC), a water heater (WH), and V2H technology, aims to minimize daily costs. The member's load includes fixed and flexible components, the latter depending on BIS, AC, WH, and electric vehicles (EVs). At the end of this level, members communicate to the EC operator and retailer whether they have a power surplus or shortage that was not addressed via P2P transactions.
2) *Second Level:* At this level, EC operators are modeled with BIS, AC, and WH systems, enabling bidirectional power exchanges with the retailer and EC members within their service area. EC operators are responsible for supplying the community's public load, which consists of fixed components (e.g., lighting) and variable components (e.g., pool heating and cooling). Their objective is to minimize daily expenses. At the end of this level, EC operators determine the power transactions required with the retailer and members within their service area.
3) *Third Level:* At this level, the retailer is modeled with the capability to conduct bidirectional power exchanges with the wholesale market (WSM), EC operators, and members. In addition, the retailer can directly procure power from distribution-level RESs. The retailer's objective is to maximize its daily profit in the market. Upon completing this level, the retailer reports the power exchange schedules at the nodes associated with EC operators, RESs, and the WSM to the DSO.
4) *Fourth Level:* At this level, the DSO, upon receiving power exchanges' information from the retailer, executes a linear AC power flow program to check network security constraints and evaluate its feasibility. The objective is to minimize deviations from the retailer's requested

schedules. At the conclusion of this level, the operating mode is determined as green, yellow, or red. If all security constraints are met and no violations occur in the retailer's requested programs, the system operates in green mode, finalizing all schedules. If the DSO detects mismatches in power flow due to losses, the system enters yellow mode. In the presence of congestion, the system enters red mode. In both yellow and red modes, the DSO informs the retailer of new constraints, requiring adjustments in the energy market schedules. Section IV introduces a novel DSO-driven algorithm designed to coordinate market operations across different modes.

The proposed model enables EC members, operators, retailers, and DSOs to act as independent decision-makers, enhancing market flexibility, decentralization, and privacy. EC members minimize costs via P2P trading; operators offer grid services; retailers maximize market participation; DSOs ensure network security without accessing contract details.

III. Mathematical Modeling

The hierarchical four-level model is formulated as a mixed-integer linear program (MILP), with uppercase letters representing parameters and lowercase letters denoting variables.

A. Level 1 (EC Members Scheduling)

In the proposed concept, EC members perform internal scheduling to minimize daily costs while maintaining hot water and room temperatures at desired levels. Upon receiving grid service signals, they adjust these temperatures within allowable ranges and regulate V2H and BIS systems accordingly. Equation (1) defines the first-level objective function, where the first term models P2P exchanges, and the second and third terms represent interactions with the EC operator and retailer. Initially, each member disables the second and third terms and settles exchanges on the P2P platform. Then, these terms are activated to manage any residual power shortages or surpluses through the EC operator or the retailer. Excluding upstream exchanges during P2P platform participation prevents members from buying power from EC operator/retailer and reselling it on the platform, thus stopping them from acting as brokers. (2) ensures power balance for each member. $P_{h,t}^{\text{Fix}}$ represents the fixed load; $p_{h,t}^{\text{BIS}}$, $p_{h,t}^{\text{WH}}$, and $p_{h,t}^{\text{AC}}$ are the operating points of BIS, WH, and AC systems; $p_{h,ev,t}^{\text{EV},C}$ and $p_{h,ev,t}^{\text{EV},D}$ represent the power charged and discharged in EV batteries, respectively. $p_{k,h,t}^{\text{P2P}}$ and $p_{h,k,t}^{\text{P2P}}$ are the power bought and sold through the P2P platform. The variables $p_{h,t}^{\text{Shor}}$ and $p_{h,t}^{\text{Sur}}$, respectively, represent the residual power shortage and surplus that were not addressed in the P2P platform. Equation (3) uses binary variables $i_{h,t}^{\text{Shor}}$ and $i_{h,t}^{\text{Sur}}$ to limit power shortages and surpluses to the capacity of each member's metering system. These binary variables cannot be 1 simultaneously

$$Z_h^{\text{Member}} = \sum_k \sum_t \left(\pi_{k,t}^{\text{P2P}} p_{k,h,t}^{\text{P2P}} - \pi_{h,t}^{\text{P2P}} p_{h,k,t}^{\text{P2P}}\right) \Delta t + \sum_t \left(\pi_t^{\text{Op,Buy}} p_{h,t}^{\text{Op,Buy}} - \pi_t^{\text{Op,Sell}} p_{h,t}^{\text{Op,Sell}}\right) \Delta t + \sum_t \left(\pi_t^{\text{Ret,Buy}} p_{h,t}^{\text{Ret,Buy}} - \pi_t^{\text{Ret,Sell}} p_{h,t}^{\text{Ret,Sell}}\right) \Delta t \tag{1}$$

$$p_{h,t}^{\text{Shor}} - p_{h,t}^{\text{Sur}} = P_{h,t}^{\text{Fix}} + p_{h,t}^{\text{BIS}} + p_{h,t}^{\text{WH}} + p_{h,t}^{\text{AC}} + \sum_{ev} \left(p_{h,ev,t}^{\text{EV},C} - p_{h,ev,t}^{\text{EV},D}\right) - \sum_k p_{k,h,t}^{\text{P2P}} + \sum_k p_{h,k,t}^{\text{P2P}} \tag{2}$$

$$0 \le p_{h,t}^{\text{Shor}} \le P_h^{\max} i_{h,t}^{\text{Shor}} \quad , \quad 0 \le p_{h,t}^{\text{Sur}} \le P_h^{\max} i_{h,t}^{\text{Sur}}. \tag{3}$$

Algorithm 1: Pseudocode of Proposed P2P Platform.

Module 1

Clear the list of contracts $\rightarrow I^{P2P} = 0$;
Set P2P power sharing price to π_t^{MMR};
for each EC member h **do**
  Solve EC members' optoimization problem;
end for

Module 2

for each EC member h, **do**
  for each hour t, **do**
    if $(i_{h,t}^{Seller} = 1)$ **then**
      Define P2P power sharing $P_{h,t}^{P2P}$ as a new contract for seller h;
      Calculate new price based on enhanced MMR;
    end if
  end for
end for

Module 3

Activate the list of P2P contracts $\rightarrow I^{P2P} = 1$;
for each EC member h, **do**
  Solve EC members' optoimization problem;
  for each hour t, **do**
    if $(P_{k,h,t}^{P2P} \neq 0)$ **then**
      Fix accepted contracts for buyer h;
    end if
  end for
  Update the price and power of contracts;
end for

Algorithm 1 outlines the process for P2P power sharing among members within a community consisting of three modules. In Module 1, power sellers are identified by deactivating the second and third terms of the objective and setting the parameter I^{P2P}, which permits power purchases from the P2P platform, to 0. This configuration restricts power exchanges with retailers and EC operators, as well as P2P purchases, allowing only the sale of power through the P2P platform. Note that in this module, the selling price of power on the P2P platform is set to the basic MMR, which is the average of the upstream market's buy and sell prices [8]. In Module 2, sellers update their selling prices using the proposed enhanced MMR method, store their excess power in the P^{P2P} parameter, and send price-power contracts to the P2P platform. In Module 3, the I^{P2P} parameter is set to 1, enabling members to purchase power from the P2P platform. Buyer members, then, acquire the required power from the available contracts. When a contract is activated, its price-power information is updated automatically. Note that the identities of contract providers and activators remain confidential and are not disclosed on the P2P platform.

Constraints (4)–(11) define the P2P power sharing mechanism. In (4), binary variables $i_{h,t}^{\text{Seller}}$ and $i_{h,t}^{\text{Buyer}}$, along with the equipment's operating point, determine each member's hourly role. A positive net value indicates a buyer, and a negative one indicates a seller; both variables cannot be 1 simultaneously. Constraint (5) enforces this exclusivity, while (6) limits power activation from contracts. Members use (7)–(11) for dynamic pricing of their excess power based on an enhanced MMR method. The basic MMR, formulated in (7) [8], sets the P2P selling price as the simple average of the upstream market's buy ($\pi_t^{\text{Ret,Buy}}$) and sell ($\pi_t^{\text{Ret,Sell}}$) prices, disregarding the seller's available energy and prior transactions. In contrast, the enhanced MMR, detailed in (8), introduces a dynamic pricing mechanism that adjusts rates based on the seller's available capacity and unfulfilled contracts, incentivizing market participation. This method ensures that sellers always receive prices at or above the basic MMR rate, while buyers never pay more than the upstream market price. Net generation and consumption are computed in (9) and (10). The enhanced MMR is designed such that as the available power per contract ($p_{h,t}^{\text{P2P,Available}}$) decreases, the $\pi_{h,t}^{\text{P2P}}$ price increases, and vice versa. The available power per contract is updated in (11) using the previous contract's total ($P_{h,t}^{\text{P2P}}$) and activated ($\sum_k p_{h,k,t}^{\text{P2P}}$) portions

$$-P_h^{\max} i_{h,t}^{\text{Seller}} \le P_{h,t}^{\text{Fix}} + p_{h,t}^{\text{BIS}} + p_{h,t}^{\text{WH}} + p_{h,t}^{\text{AC}} + \sum_{ev}\left(p_{h,ev,t}^{\text{EV},C} - p_{h,ev,t}^{\text{EV},D}\right) \le P_h^{\max} i_{h,t}^{\text{Buyer}} \tag{4}$$

$$\sum_k p_{k,h,t}^{\text{P2P}} \le P_h^{\max} i_{h,t}^{\text{Buyer}} I^{\text{P2P}}, \quad \sum_k p_{h,k,t}^{\text{P2P}} \le P_h^{\max} i_{h,t}^{\text{Seller}} \tag{5}$$

$$0 \le p_{k,h,t}^{\text{P2P}} \le P_{k,t}^{\text{P2P}} i_{k,h,t}^{\text{P2P}} \tag{6}$$

$$\pi_t^{\text{MMR}} = \frac{\pi_t^{\text{Ret,Buy}} + \pi_t^{\text{Ret,Sell}}}{2} \tag{7}$$

$$\pi_{h,t}^{\text{P2P}} = \frac{\pi_t^{\text{Ret,Buy}} p_{h,t}^{D} + \pi_t^{\text{MMR}} p_{h,t}^{\text{Available}}}{p_{h,t}^{G}} \tag{8}$$

$$p_{h,t}^{D} = P_{h,t}^{\text{Fix}} + p_{h,t}^{B,C} + p_{h,t}^{\text{WH}} + p_{h,t}^{\text{AC}} + \sum_{ev} p_{h,ev,t}^{\text{EV},C} + \sum_k p_{h,k,t}^{\text{P2P}} \tag{9}$$

$$p_{h,t}^{G} = p_{h,t}^{B,D} + P_{h,t}^{\text{SP}} + \sum_{ev} p_{h,ev,t}^{\text{EV},D} \tag{10}$$

$$p_{h,t}^{\text{P2P,Available}} = P_{h,t}^{\text{P2P}} - \sum_k p_{h,k,t}^{\text{P2P}}. \tag{11}$$

Equation (12) states that each member can manage its power shortage/surplus not addressed on the P2P platform through exchanges with the retailer and EC operator. The restrictions on power exchanges with the EC operator are presented in (13) and (14), while restrictions on power exchanges with the retailer are presented in (15) and (16). $\gamma_{h,t}^{\text{Buy,ECO}\to\text{ECM}}/\gamma_{h,t}^{\text{Sell,ECO}\to\text{ECM}}$ and $\gamma_{i=N_c,t}^{\text{Limit,Buy}}/\gamma_{i=N_c,t}^{\text{Limit,Sell}}$ are restrictions imposed by the EC operator and retailer on member exchanges, ranging from 0 to 1 in the optimization. A value of 1 indicates no limit on exchanges, with each decrement of 0.01 representing a 1% restriction on nodal power exchanges. Binary variables representing buying ($i_{h,t}^{\text{Op,Buy}}/i_{h,t}^{\text{Ret,Buy}}$) and selling ($i_{h,t}^{\text{Op,Sell}}/i_{h,t}^{\text{Ret,Sell}}$) cannot be 1 simultaneously. In the proposed concept, each member exchanges up to 2 kW exclusively with the EC operator. For amounts above 2 kW, exchanges with both the EC operator and the retailer are allowed, with preference given to the retailer due to more favorable pricing

$$p_{h,t}^{\text{Shor}} - p_{h,t}^{\text{Sur}} = \left(p_{h,t}^{\text{Op,Buy}} - p_{h,t}^{\text{Op,Sell}}\right) + \left(p_{h,t}^{\text{Ret,Buy}} - p_{h,t}^{\text{Ret,Sell}}\right) \tag{12}$$

$$0 \le p_{h,t}^{\text{Op,Buy}} \le P_{h,t}^{\text{Op-Buy,max}} i_{h,t}^{\text{Op,Buy}} \gamma_{h,t}^{\text{Buy,ECO}\to\text{ECM}} \tag{13}$$

$$0 \le p_{h,t}^{\text{Op,Sell}} \le P_{h,t}^{\text{Op-Sell,max}} i_{h,t}^{\text{Op,Sell}} \gamma_{h,t}^{\text{Sell,ECO}\to\text{ECM}} \tag{14}$$

$$P^{\text{Ret,min}} i_{h,t}^{\text{Ret,Buy}} \le p_{h,t}^{\text{Ret,Buy}} \le P_{h,t}^{\text{Ret-Buy,max}} i_{h,t}^{\text{Ret,Buy}} \gamma_{i=N_c,t}^{\text{Limit,Buy}} \tag{15}$$

$$p^{\text{Ret,min}} i_{h,t}^{\text{Ret,Sell}} \le p_{h,t}^{\text{Ret,Sell}} \le P_{h,t}^{\text{Ret-Sell,max}} i_{h,t}^{\text{Ret,Sell}} \gamma_{i=N_c,t}^{\text{Limit,Sell}}. \tag{16}$$

Equation (17)–(20) model the WH system: (17) determines the hourly water temperature, where $\theta_{h,t-1}^{W}$, $p_{h,t}^{\text{WH}}$, $m_{h,t}^{\text{WH}}$, $m_{h,t}^{\text{Loss}}$, $D_{h,t}^{W}$, and ξ represent the previous hour's temperature, power consumption, energy required to heat incoming water, energy losses, hot water demand, and the water thermal constant. Equation (18) restricts temperature variations. Equation (19) computes the energy required to heat incoming water. Equation (20) calculates hourly losses based on current water temperature ($\theta_{h,t}^{W}$), outdoor temperature ($\theta_{h,t}^{\text{Out}}$), and tank characteristics, where S_h^{Surface}, X, σ, and H represent the tank area, insulation thickness, thermal conductivity, and surface heat transfer coefficient. Equation (21) and (22) model the AC system: (21) determines indoor temperature, influenced by the AC operating point ($p_{h,t}^{\text{AC}}$), with $\theta_{h,t}^{\text{Out}}$, $\theta_{h,t-1}^{\text{In}}$, α^{AC}, and α^{Wall} representing outdoor temperature, previous indoor temperature, AC efficiency, and wall thermal factor. Equation (22) confines indoor temperature. Equation (23) constrains WH and AC power consumption, while (24) quantifies thermal comfort.

$$\theta_{h,t}^{W} = \theta_{h,t-1}^{W} + \frac{p_{h,t}^{\text{WH}}\Delta t - m_{h,t}^{\text{WH}} - m_{h,t}^{\text{Loss}}}{\xi D_{h,t}^{W}} \tag{17}$$

$$\theta_{h,t=0}^{W} = \theta_h^{W,\text{Initial}}, \quad \theta_{h,t}^{W,\min} \le \theta_{h,t}^{W} \le \theta_{h,t}^{W,\max} \tag{18}$$

$$m_{h,t}^{WH} = \xi D_{h,t}^{W}\left(\theta_{h,t}^{W} - \theta^{\text{Incoming}}\right) \tag{19}$$

$$m_{h,t}^{\text{Loss}} = \frac{\theta_{h,t}^{W} - \theta_t^{\text{Out}}}{\frac{X}{\sigma} + \frac{1}{H}} S_h^{\text{Surface}} \Delta t \tag{20}$$

$$\theta_{h,t}^{\text{In}} = \left(1 - \alpha^{\text{Wall}}\right)\theta_{h,t-1}^{\text{In}} + \alpha^{\text{Wall}}\theta_t^{\text{Out}} + \alpha^{\text{AC}} p_{h,t}^{\text{AC}} \Delta t \tag{21}$$

$$\theta_{h,t=0}^{\text{In}} = \theta_h^{\text{In,Initial}}, \quad \theta_{h,t}^{\text{In,min}} \le \theta_{h,t}^{\text{In}} \le \theta_{h,t}^{\text{In,max}} \tag{22}$$

$$m_{h,t}^{\text{WH}} \le p_{h,t}^{\text{WH}} \Delta t \le M_{h,t}^{\text{WH,max}}, \quad 0 \le p_{h,t}^{\text{AC}} \le P_h^{\text{AC,max}} \tag{23}$$

$$\Omega_{h,t}^{\text{TC}} = 100 - \left(\varepsilon\left|\theta^{\text{In,Pref}} - \theta_{h,t}^{\text{In}}\right| + \varepsilon\left|\theta^{W,} - \theta_{h,t}^{W}\right|\right). \tag{24}$$

EVs of EC members provide V2H services, as modeled in (25)–(29). Equation (25) updates the EV battery's energy based on the previous hour and current charging/discharging. Equation (26) defines its energy at the schedule's start and end, while (27) sets hourly limits. Equation (28) restricts charging/discharging rates. Equation (29) links these operations to the EV's presence via $I^{\text{Parking}}_{h,ev,t}$.

$$e^{\text{EV}}_{h,ev,t} = e^{\text{EV}}_{h,ev,t-1} + \left(\eta^{\text{EV},C} p^{\text{EV},C}_{h,ev,t} - \frac{p^{\text{EV},D}_{h,ev,t}}{\eta^{\text{EV},D}}\right)\Delta t \tag{25}$$

$$e^{\text{EV}}_{h,ev,t=T^{Ar}_{h,ev}} = E^{\text{EV,Initial}}_{h,ev} \quad , \quad e^{\text{EV}}_{h,ev,t=T^{Dp}_{h,ev}} \geq E^{\text{EV,Final}}_{h,ev} \tag{26}$$

$$E^{\text{EV,min}}_{h,ev} \leq e^{\text{EV}}_{h,ev,t} \leq E^{\text{EV,max}}_{h,ev} \tag{27}$$

$$\begin{aligned} 0 \leq p^{\text{EV},C}_{h,ev,t} &\leq P^{C,\max}_{h,ev,t} i^{\text{EV},C}_{h,ev,t}, \\ 0 \leq p^{\text{EV},D}_{h,ev,t} &\leq P^{D,\max}_{h,ev,t} i^{\text{EV},D}_{h,ev,t} \end{aligned} \tag{28}$$

$$i^{\text{EV},C}_{h,ev,t} + i^{m,D}_{h,ev,t} \leq I^{\text{Parking}}_{h,ev,t}. \tag{29}$$

The BIS system is modeled in (30)–(35). Equation (30) determines solar panel output, (31) defines battery energy levels, and (32) sets the schedule's start and end levels. Equation (33) limits charging and discharging, while (34) imposes energy bounds. Equation (35) ensures the power balance of the BIS system.

$$p^{\text{SP}}_{h,t} = \eta^{\text{SP}} \frac{R_t}{R^{\text{STC}}} P^{\text{SP,max}}_{h} \tag{30}$$

$$e^{B}_{h,t} = e^{B}_{h,t-1} + \left(\eta^{B,C} p^{B,C}_{h,t} - \frac{p^{B,D}_{h,t}}{\eta^{B,D}}\right)\Delta t \tag{31}$$

$$e^{B}_{h,t=0} = E^{B,\text{Initial}}_{h} \quad , \quad e^{B}_{h,t=T} = E^{B,\text{Initial}}_{h} \tag{32}$$

$$0 \leq p^{B,C}_{h,t} \leq P^{C,\max}_{h} i^{B,C}_{h,t} \ , \ 0 \leq p^{B,D}_{h,t} \leq P^{D,\max}_{h} i^{B,D}_{h,t} \tag{33}$$

$$E^{B,\min}_{h} \leq e^{B}_{h,t} \leq E^{B,\max}_{h} \tag{34}$$

$$p^{\text{BIS}}_{h,t} = p^{B,C}_{h,t} - p^{B,D}_{h,t} - P^{\text{SP}}_{h,t}. \tag{35}$$

B. Level 2 (EC Operators Scheduling)

In (36), the second-level objective function aims to minimize each EC operator's expenses. The first and second terms model the net exchanges of EC operator with members within its service area and the retailer, respectively, while the third term represents the imbalance penalty incurred due to the inability to address the exchanges requested by the members. Without exchange limits, the EC operator fulfills all member requests, keeping $p^{Imb,\text{Buy}}_{c,t}$ and $p^{Imb,\text{Sell}}_{c,t}$ at zero. With imposed limits, some requests may be unmet, leading to imbalances and nonzero values for these variables. The EC operator updates member exchange limits in (37) and (38), assigning values between zero and one. Constraint (39) limits EC operators' exchange with the retailer, with DSO-informed restrictions dynamically adjusting the upper bound. Finally, (40) defines the EC operator's power balance.

$$\begin{aligned} Z^{Op}_{c} = &\sum_{h\in\Theta^h_c}\sum_{t}\left(\pi^{\text{Op,Sell}}_{t} P^{\text{Op,Sell}}_{h,t} - \pi^{\text{Op,Buy}}_{t} P^{\text{Op,Buy}}_{h,t}\right) \\ &\times \Delta t + \sum_{t}\left(\pi^{\text{Ret,Buy}}_{t} p^{\text{Ret,Buy}}_{c,t} - \pi^{\text{Ret,Sell}}_{t} p^{\text{Ret,Sell}}_{c,t}\right) \\ &\times \Delta t + \pi^{\text{Imb}} \sum_{t}\left(p^{\text{Imb,Buy}}_{c,t} + p^{\text{Imb,Sell}}_{c,t}\right)\Delta t \end{aligned} \tag{36}$$

$$\gamma^{\text{Buy,ECO}\to\text{ECM}}_{h\in\Theta^h_c,t} = \frac{\sum_{h\in\Theta^h_c} P^{\text{Op,Buy}}_{h,t} - p^{\text{Imb,Buy}}_{c,t}}{\sum\limits_{h\in\Theta^h_c} P^{\text{Op,Buy}}_{h,t}} \tag{37}$$

$$\gamma^{\text{Sell,ECO}\to\text{ECM}}_{h\in\Theta^h_c,t} = \frac{\sum\limits_{h\in\Theta^h_c} P^{\text{Op,Sell}}_{h,t} - p^{\text{Imb,Sell}}_{c,t}}{\sum\limits_{h\in\Theta^h_c} P^{\text{Op,Sell}}_{h,t}} \tag{38}$$

$$\begin{aligned} 0 \leq p^{\text{Ret,Buy}}_{c,t} &\leq P^{\text{Ret}-\text{Buy},\max}_{c,t} i^{\text{Ret,Buy}}_{c,t} \gamma^{\text{Limit,Buy}}_{i=N_c,t} \\ 0 \leq p^{\text{Ret,Sell}}_{c,t} &\leq P^{\text{Ret}-\text{Sell},\max}_{c,t} i^{\text{Ret,Sell}}_{c,t} \gamma^{\text{Limit,Sell}}_{i=N_c,t} \end{aligned} \tag{39}$$

$$\begin{aligned} &p^{\text{Ret,Buy}}_{c,t} - p^{\text{Ret,Sell}}_{c,t} + p^{\text{Imb,Buy}}_{c,t} - p^{\text{Imb,Sell}}_{c,t} \\ &= \sum_{h\in\Theta^h_c}\left(P^{\text{Op,Buy}}_{h,t} - P^{\text{Op,Sell}}_{h,t}\right) + P^{\text{Fix}}_{c,t} \\ &\quad + p^{\text{BIS}}_{c,t} + p^{WH}_{c,t} + p^{\text{AC}}_{c,t}. \end{aligned} \tag{40}$$

C. Level 3 (Retailer Scheduling)

At the third level, the retailer aims to maximize profit from market transactions, as shown in (41). The first to fifth terms represent exchanges with the WSM, EC operators, EC members, fixed grid loads, and RESs, respectively. The retailer's power balance is enforced by (42). The parameter α^{Loss} is set to 1in yellow mode to activate the loss term ($P^{\text{Loss,Total}}_{t}$) in the retailer's power balance. In other modes, $\alpha^{\text{Loss}} = 0$, as the retailer lacks access to power flow constraints and receives loss information only from the DSO in yellow mode. Equation (43) limits the retailer's exchanges with the WSM based on DSO restrictions. In (44), the retailer calculates and stores net hourly generation/consumption for each node in $p^{\text{Gen}}_{i=N_c,t}$ and $p^{\text{Con}}_{i=N_c,t}$. This allows the retailer to avoid sharing contract details with the DSO, instead providing only the net hourly generation/consumption of each node.

$$\begin{aligned} Z^{\text{Ret}} = &\sum_{t}\left(\pi^{\text{WSM,Sell}}_{t} p^{\text{WSM,Sell}}_{t} - \pi^{\text{WSM,Buy}}_{t} p^{\text{WSM,Buy}}_{t}\right)\Delta t \\ &+ \sum_{c}\sum_{t}\left(\pi^{\text{Ret,Buy}}_{t} p^{\text{Ret,Buy}}_{c,t} - \pi^{\text{Ret,Sell}}_{t} p^{\text{Ret,Sell}}_{c,t}\right)\Delta t \\ &+ \sum_{h}\sum_{t}\left(\pi^{\text{Ret,Buy}}_{t} p^{\text{Ret,Buy}}_{h,t} - \pi^{\text{Ret,Sell}}_{t} p^{\text{Ret,Sell}}_{h,t}\right)\Delta t \\ &+ \sum_{i}\sum_{t}\left(p^{\text{WSM,Buy}}_{t} P^{\text{Fixed,Load}}_{i,t}\right)\Delta t \end{aligned}$$

$$-\sum_{t}\sum_{sp}\left(\pi_{sp}^{\mathrm{SP}}p_{sp,t}^{\mathrm{SP}}\right)\Delta t-\sum_{t}\sum_{wt}\left(\pi_{wt}^{WT}p_{wt,t}^{WT}\right)\Delta t \tag{41}$$

$$p_t^{\mathrm{WSM,Buy}}-p_t^{\mathrm{WSM,Sell}}+\sum_{sp}p_{sp,t}^{\mathrm{SP}}+\sum_{wt}p_{wt,t}^{\mathrm{WT}}+\sum_{i}p_{i,t}^{\mathrm{Gen}}$$
$$=\sum_{t}P_{i,t}^{\mathrm{Fixed,Load}}+\sum_{i}p_{i,t}^{\mathrm{Con}}+\alpha^{\mathrm{Loss}}P_t^{\mathrm{Loss,Total}} \tag{42}$$

$$0\le p_t^{\mathrm{WSM,Buy}}\le P^{\mathrm{WSM,max}}i_t^{\mathrm{WSM,Buy}}$$
$$0\le p_t^{\mathrm{WSM,Sell}}\le P^{\mathrm{WSM,max}}i_t^{\mathrm{WSM,Sell}} \tag{43}$$

$$\begin{cases}p_{i=N_c,t}^{\mathrm{Gen}}=P_{c,t}^{\mathrm{Ret,Sell}}+\sum_{h\in\Theta_c^h}p_{h,t}^{\mathrm{Ret,Sell}}\\ p_{i=N_c,t}^{\mathrm{Con}}=P_{c,t}^{\mathrm{Ret,Buy}}+\sum_{h\in\Theta_c^h}p_{h,t}^{\mathrm{Ret,Buy}}.\end{cases} \tag{44}$$

D. Level 4 (DSO Scheduling)

The DSO objective function, detailed in (45), minimizes deviations from retailer-requested programs and load shedding while ensuring network security. Letters without a bar represent retailer-requested programs, while those with a bar denote DSO-obtained programs. The penalty coefficients β^{WSM}, β^{Gen}, and β^{Con} are set to 1, 1.1, and 1.2, respectively, to enforce minimal deviations from retailer-requested programs. If no deviations occur, the objective function remains zero; otherwise, it becomes positive based on the magnitude of deviations and corresponding weight coefficients. The penalty β^{Shed}, assigned the highest weight of 4, ensures that the DSO resorts to load shedding only when power flow issues cannot be resolved through adjustments to retailer-requested programs. Equation (46) and (47) ensure nodal balance of active and reactive power, while (48) links reactive power to active power. (49) and (50) calculate active and reactive power flow, respectively, and (51) calculates line losses. Quadratic terms $(p_{l,t}^{\mathrm{Line}})^2$ and $(q_{l,t}^{\mathrm{Line}})^2$ are linearized via the piecewise technique. Using (51), the DSO also computes hourly network power losses and informs the retailer to increase WSM purchases to compensate. Equation (52) presents the security constraint for power flow. Equation (53) restricts the voltage magnitude and phase angle variables within predefined limits to ensure feasible power flow. As per (54), the DSO updates nodal restrictions based on its own ($\bar{p}_{i,t}^{\mathrm{Gen}}/\bar{p}_{i,t}^{\mathrm{Con}}$) and the retailer's ($P_{i,t}^{\mathrm{Gen}}/P_{i,t}^{\mathrm{Con}}$) optimized programs, and informs the retailer. If the requested programs are approved, no restrictions apply; otherwise, they are assigned a value greater than 0 and up to 1.

$$Z^{\mathrm{DSO}}=\overbrace{\beta^{\mathrm{WSM}}\sum_{t}\left(\left|\bar{p}_t^{\mathrm{WSM,Buy}}-P_t^{\mathrm{WSM,Buy}}\right|+\left|\bar{p}_t^{\mathrm{WSM,Sell}}-P_t^{\mathrm{WSM,Sell}}\right|\right)\Delta t}^{\mathrm{Part}_1}$$
$$+\overbrace{\beta^{\mathrm{Gen}}\sum_{i\in N_c}\sum_{t}\left|\bar{p}_{i,t}^{\mathrm{Gen}}-P_{i,t}^{\mathrm{Gen}}\right|\Delta t+\beta^{\mathrm{Con}}\sum_{i\in N_c}\sum_{t}\left|\bar{p}_{i,t}^{\mathrm{Con}}-P_{i,t}^{\mathrm{Con}}\right|\Delta t}^{\mathrm{Part}_2}$$
$$+\overbrace{\beta^{\mathrm{Shed}}\sum_{i}\sum_{t}P_{i,t}^{\mathrm{Shed,Load}}\Delta t}^{\mathrm{Part}_3} \tag{45}$$

$$\bar{p}_t^{\mathrm{WSM,Buy}}\Big|_{i=1}-\bar{p}_t^{\mathrm{WSM,Sell}}\Big|_{i=1}+\sum_{sp\in\Theta_i^{sp}}p_{sp,t}^{\mathrm{SP}}+\sum_{wt\in\Theta_i^{wt}}p_{wt,t}^{\mathrm{WT}}$$
$$+\bar{p}_{i=N_c,t}^{\mathrm{Gen}}=P_{i,t}^{\mathrm{Fixed,Load}}-P_{i,t}^{\mathrm{Shed,Load}}$$
$$+\bar{p}_{i=N_c,t}^{\mathrm{Con}}+\sum_{l\in\Theta_i^l}\left(\tau_{l,i}^{\mathrm{Line}}p_{l,t}^{\mathrm{Line}}+\frac{p_{l,t}^{\mathrm{Loss}}}{2}S^{\mathrm{Base}}\right) \tag{46}$$

$$q_t^{\mathrm{WSM,Buy}}\Big|_{i=1}+\bar{q}_{i=N_c,t}^{\mathrm{Gen}}=Q_{i,t}^{\mathrm{Fixed,Load}}-PF_iP_{i,t}^{\mathrm{Shed,Load}}$$
$$+\bar{q}_{i=N_c,t}^{\mathrm{Con}}+\sum_{l\in\Theta_i^l}\left(\tau_{l,i}^{\mathrm{Line}}q_{l,t}^{\mathrm{Line}}\right) \tag{47}$$

$$\bar{q}_{i=N_c,t}^{\mathrm{Gen}}=PF_i\bar{p}_{i=N_c,t}^{\mathrm{Gen}}\ ,\ \bar{q}_{i=N_c,t}^{\mathrm{Con}}=PF_i\bar{p}_{i=N_c,t}^{\mathrm{Con}} \tag{48}$$

$$\frac{p_{l,t}^{\mathrm{Line}}}{S^{\mathrm{Base}}}=G_l\left(v_{i,t}-v_{j,t}\right)+B_l\left(\delta_{i,t}-\delta_{j,t}\right) \tag{49}$$

$$\frac{q_{l,t}^{\mathrm{Line}}}{S^{\mathrm{Base}}}=B_l\left(v_{i,t}-v_{j,t}\right)-G_l\left(\delta_{i,t}-\delta_{j,t}\right) \tag{50}$$

$$p_{l,t}^{\mathrm{Loss}}=\frac{R_l\left[\left(p_{l,t}^{\mathrm{Line}}\right)^2+\left(q_{l,t}^{\mathrm{Line}}\right)^2\right]}{\left(S^{\mathrm{Base}}\right)^2}\ ,\ P_t^{\mathrm{Loss,Total}}=\sum_{l}P_{l,t}^{\mathrm{Loss}} \tag{51}$$

$$\left(p_{l,t}^{\mathrm{Line}}\right)^2+\left(q_{l,t}^{\mathrm{Line}}\right)^2\le\left(S_l^{\mathrm{Line,max}}\right)^2 \tag{52}$$

$$V^{\min}\le v_{i,t}\le V^{\max}\ ,\ \theta^{\min}\le\theta_{i,t}\le\theta^{\max} \tag{53}$$

$$\gamma_{i,t}^{\mathrm{Limit,Buy}}=\frac{\bar{p}_{i,t}^{\mathrm{Con}}}{P_{i,t}^{\mathrm{Con}}}\ ,\ \gamma_{i,t}^{\mathrm{Limit,Sell}}=\frac{\bar{p}_{i,t}^{\mathrm{Gen}}}{P_{i,t}^{\mathrm{Gen}}}. \tag{54}$$

E. Risk Management

In the proposed model, EC operators and members plan under uncertainty in solar generation and load demand. To represent this uncertainty, 50 scenarios per parameter are generated using Gaussian and Beta distributions, yielding a dataset of 2500 scenarios. The ScenRed tool in GAMS reduces this to five representative scenarios for computational efficiency. A CVaR-based optimization framework, defined in (55)–(58), incorporates these scenarios for risk-aware decision-making. Equation (55) reformulates the objective functions of EC operators and members by introducing the scenario index (s), while the overall risk management objective is given in (56). This objective function minimizes the overall cost Z^{Risk}, which is a weighted combination of scenario-specific cost (Z_s) and CVaR (Z^{CVaR}). Here, ψ balances between weighted scenario costs and CVaR. ω_s denotes the probability of scenarios. (57) calculates the CVaR considering VaR (Z^{VaR}), the expected shortfall ($\sum_s(\omega_s\Delta_s)$), and the confidence level (α^{Conf}). Increasing α^{Conf}reduces the denominator, raising Z^{CVaR} and making the approach more risk-averse. Conversely, decreasing α^{Conf}enlarges the denominator,

lowering Z^{CVaR} and leading to a more risk-tolerant approach. Equation (58) ensures that the shortfall Δ_s is at least the difference between the scenario-specific cost and the VaR. Note that the shortfall is always nonnegative.

$$Z_s \in \left\{Z_{h,s}^{M}, Z_{c,s}^{\text{Op}}\right\} \tag{55}$$

$$\min Z^{\text{Risk}} = \psi \sum_{s} (\omega_s Z_s) + (1-\psi)\, Z^{\text{CVaR}} \tag{56}$$

$$Z^{\text{CVaR}} = Z^{\text{VaR}} + \frac{1}{1-\alpha^{\text{Conf}}} \sum_{s} (\omega_s \Delta_s) \tag{57}$$

$$\Delta_s \geq Z_s - Z^{\text{VaR}}. \tag{58}$$

IV. Proposed DSO-Driven Algorithm

The proposed DSO-driven algorithm is implemented according to Algorithm 2. Initially, Module 1 is executed, solving levels 1 to 3 of the model. Subsequently, level 4 is solved, wherein the DSO determines the operational mode. Since the retailer lacks access to the power flow program and network information, it cannot calculate the losses and congestion caused by the power flow, resulting in the operation always going to either yellow or red mode. If the DSO finds only a mismatch caused by losses, the operation goes to yellow mode, and the lack of power is announced to the retailer, executing Module 2. If the DSO finds line congestion, the operation goes into red mode, and new power exchange restrictions are announced to the retailer, executing Module 3.

In yellow mode, according to Module 2, only the third and fourth levels are solved. The retailer purchases the power shortage from the WSM and sends the updated exchanges to the DSO for feasibility checks. If no congestion is found, the operation transitions to green mode, finalizing all exchanges. Otherwise, new constraints are applied to eliminate congestion, and the operation transitions to red mode.

In red mode, according to Module 3, first to third levels of the proposed model are resolved, rescheduling all market parties according to the new restrictions. Since the new exchanges consider the DSO's restrictions, there will be no more congestion. The DSO calculates the losses from the updated exchanges using the power flow program, informs the retailer, and executes Module 2 to address the power losses. Since the congestion issues have already been resolved and the loss issues will be addressed by executing Module 2, the operation will transition to green mode, and the algorithm will terminate.

The proposed DSO-driven algorithm ensures convergence regardless of problem size by iteratively refining power exchange signals, meeting network constraints without excessive computations. Its hierarchical structure enhances computational efficiency by decomposing the problem into four levels, reducing problem size and ensuring decentralized decision-making, while avoiding the computational burden of centralized optimization and the slow convergence of fully distributed methods. Although no encryption technology is implemented, privacy is preserved through aggregated net transaction reporting: The DSO receives only the total power exchanged at each node, without access to individual contract details. The DSO calculates nodal restrictions and communicates them to the retailer, who, having access to individual exchange data, informs the relevant agents accordingly. This ensures effective coordination while maintaining participant privacy.

Algorithm 2: Pseudocode of the DSO-Driven Algorithm.

1: **for** each iteration $iter$, **do** — **Module 1**

2: **while** (1) **do**
3: **Run** P2P power sharing process (Algorithm 1);
4: **Set** run status to 1 for all ECs $\rightarrow Run_c^{Level\ 2} = 1$;
5: **for** each EC operator c, **do**
6: **if** $(Run_c^{Level\ 2} = 1)$ **then**
7: **Solve** optoimization problem of EC c;
8: **Check & Save** exchange imbalances within EC c $\rightarrow p_{c,t}^{Imb,Buy}$, $p_{c,t}^{Imb,Sell}$;
9: **end if**
10: **if** $\left(\sum_c \sum_t (p_{c,t}^{Imb,Buy} + p_{c,t}^{Imb,Sell}) = 0\right)$ **then**
11: **Set** run status to 0 for EC $c \rightarrow Run_c^{Level\ 2} = 0$;
12: **else**
13: **Send** restrictions to EC members $\rightarrow \gamma_{h,t}^{Buy,ECO\rightarrow ECM}$, $\gamma_{h,t}^{Sell,ECO\rightarrow ECM}$;
14: **end if**
15: **end for**
16: **if** $\left(\sum_c Run_c^{Level\ 2} = 0\right)$ **then**
17: **Break**;
18: **end if**
19: **end while**
20: **Set** loss factor to $0 \rightarrow \alpha^{Loss} = 0$;
21: **Solve** retailer's optoimization problem;
22: **Solve** DSO's optoimization problem;
23: **if** $(Part_1 + Part_2 = 0)$ **then**
24: Operation enters Green mode;
25: **Break**;
26: **end if**

Module 2

27: **if** $(Part_1 + Part_2 \neq 0)$ **then**
28: **if** $(Part_1 > 0\ \&\ Part_2 = 0)$ **then**
29: Operation enters Yellow mode;
30: **Calculate** hourly power losses and communicate signals to the retailer $\rightarrow P_t^{Loss,Total}$;
31: **Set** loss factor to $1 \rightarrow \alpha^{Loss} = 1$;
32: **GoTo** line (21) $\rightarrow$ Level 3;
33: **end if**
34: **end if**

Module 3

35: **if** $(Part_1 + Part_2 \neq 0)$ **then**
36: **if** $(Part_2 > 0)$ **then**
37: Operation enters Red mode;
38: **Calculate** restrictions for coupling nodes with ECs $\rightarrow \gamma_{i=node,t}^{Limit,Buy}$, $\gamma_{i=node,t}^{Limit,Sell}$;
39: **GoTo** line (2) $\rightarrow$ Level 1;
40: **end if**
41: **end if**

42: **end for**

V. Simulation Results

The proposed model was tested on a 594-node distribution network in Victoria, Australia, with 27 ECs, as shown in Fig. 2. Coded in GAMS and solved with CPLEX, the model was implemented on a laptop with a Core i7 processor and 12 GB RAM and evaluated through three case studies. Input data are in [22]. The numerical results for Cases 1 to 3 are shown in Table II. The model converged in 463.8, 955.7, and 1275.6 s for Cases 1, 2, and 3, respectively. Case 1, without the P2P platform and internal controllable technologies, was the fastest, while

TABLE II
NUMERICAL OUTCOMES OF CASE STUDIES

Cases	EC members' transactions ($)			EC operators' transactions ($)			Retailer's transactions ($)					Solution Time (s)
	EC Op.	Retailer	Sum	EC Mem.	Retailer	Sum	EC Mem.	EC Op.	RESs	WSM	Sum	
Case 1	5854.94	37 735.12	43 590.06	−5854.94	3998.39	−1856.55	−37 735.12	−3998.39	2217.82	37971	−1544.69	463.8
Case 2	871.93	38 817.28	39 689.21	−871.93	2631.1	1759.17	−38 817.28	−2631.1	2217.82	37 958.26	−1272.3	955.7
Case 3	2761.61	33 948.93	36 710.54	−2761.61	2354.83	−406.78	−33 948.93	−2354.83	2217.82	33 798.22	−287.72	1275.6

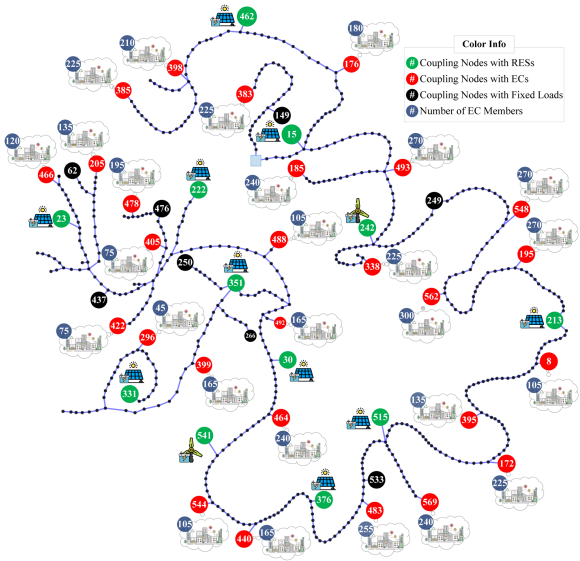

Fig. 2. Modified 594-node case study in Victoria, Australia.

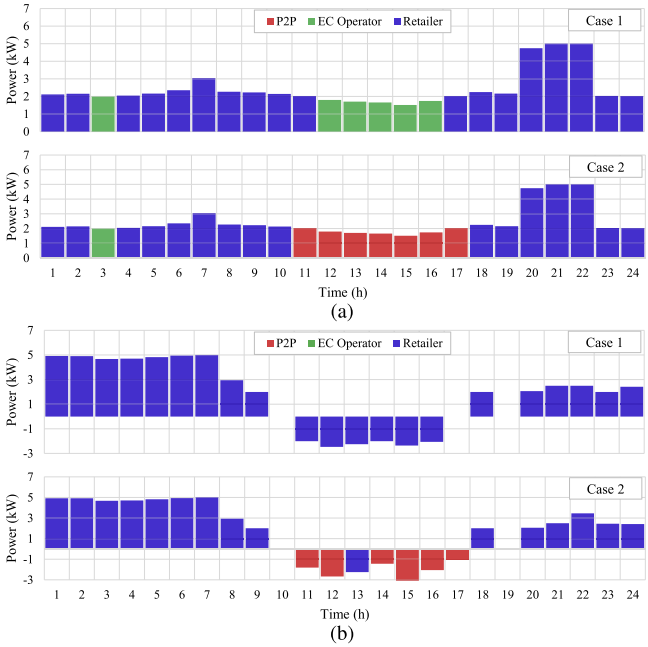

Fig. 3. Power exchange analysis of EC member types A and B. (a) EC member type A. (b) EC member type B.

Case 3, with both activated, was the slowest. Nevertheless, all solution times remain well within practical limits for day-ahead market applications.

In Case 1, EC members do not have access to the P2P platform, whereas in Case 2, they do. The results indicate that without P2P access (Case 1), members' payments to EC operators increased by $4983.01, and total daily costs rose by 9.82% compared to Case 2. Fig. 3(a) and (b) analyze the power exchanges of two different members: One is always a power buyer (type A), and the other is both a power buyer and seller (type B). Fig. 3(a) shows that in Case 2, the member who was always a power buyer purchased a total of 58.14 kWh at a cost of $10.13, with 12.45 kWh from the P2P platform, 1.99 kWh from the EC operator, and 43.7 kWh from the retailer. In Case 1, due to the lack of access to the P2P platform, this member had to rely entirely on the EC operator and retailer, increasing costs by 36.22%, compared to Case 2. Fig. 3(b) illustrates that the member acting as both buyer and seller in Case 2 sold 12.29 kWh via the P2P platform, earning a profit of $2.1. In Case 1, without P2P access, the member sold all surplus to the retailer for $2, resulting in a 4.76% profit reduction. These results confirm that the proposed P2P structure with enhanced MMR pricing reduces daily costs for both buyers and sellers.

Fig. 4(a) and (b) compare P2P prices from the basic MMR with the initial and updated prices from the enhanced MMR. P2P selling prices under the enhanced MMR consistently exceed

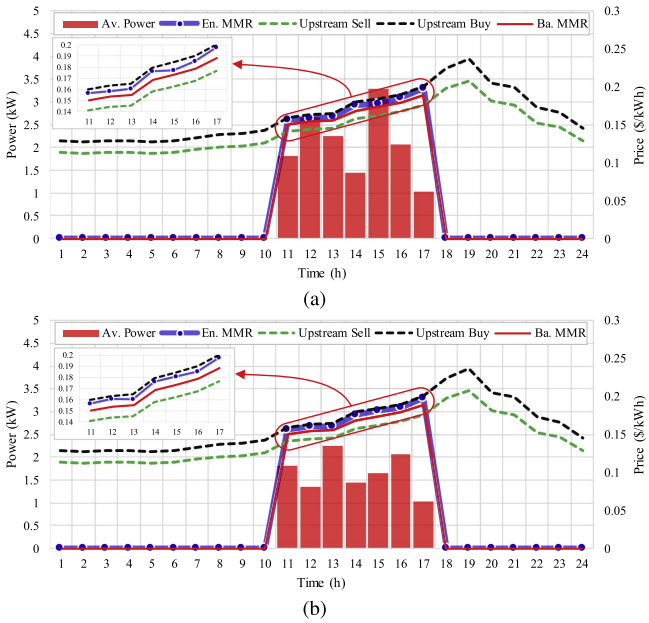

Fig. 4. Contracts from an EC member on the P2P platform. (a) Initial contracts (first iteration). (b) Updated contracts (second iteration).

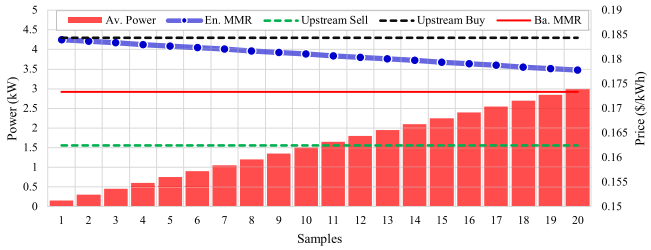

Fig. 5. Sensitivity of MMR prices to member's available power.

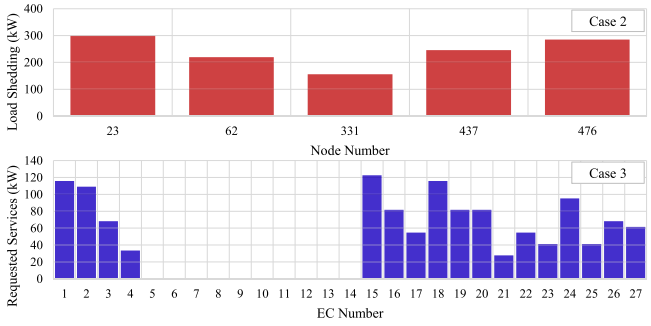

Fig. 6. Downward services used to eliminate congestions.

those of the basic MMR, favoring sellers, while purchase prices remain below upstream market rates, benefiting buyers. The basic MMR yields static prices based on average upstream purchase and sale prices. In contrast, the enhanced MMR generates dynamic prices that rise as a member's available power decreases. Notably, following initial contract activation, reduced available power leads to higher prices in the second iteration. Notably, the EC member's profit in the P2P market increased from $2.4 under the basic MMR to $2.52 under the enhanced MMR, a 4.91% improvement, as selling prices were set closer to upstream market boundaries. The analysis of settlement time on the P2P platform within an EC connected to node 562, consisting of 300 members, shows that the enhanced MMR, despite its more complex and dynamic pricing mechanism, reaches a solution in 76.1 s, only 1.6% slower than the basic MMR, which settles in 74.9 s. This confirms that the enhanced MMR ensures P2P seller profitability without delaying market settlement. Fig. 5 presents a sensitivity analysis of the member's available power on prices computed by the basic and enhanced MMR methods. The basic MMR yields a constant price across all 20 available power levels, while the enhanced MMR shows a decreasing trend. Specifically, its price drops by 3.38% as the available power increases from 0.15 kW (step 1) to 3 kW (step 20), demonstrating sensitivity to power availability.

Case 3 builds on Case 2 by enabling ECs to provide grid services using BIS, TCLs, and V2H technologies. Under congestion, EC members and operators are allowed to deviate from preferred water (55 °C ± 5 °C) and room (22 °C ± 2 °C) temperatures. Additional flexibility is also provided through storage and V2H systems. Numerical results show that these services reduced EC members' total costs by 7.5% compared to Case 2. Fig. 6 shows the capacities used by the DSO to relieve congestion at 7:00 A.M. in Cases 2 and 3. In Case 2, the lack of EC grid services caused load shedding at interruptible

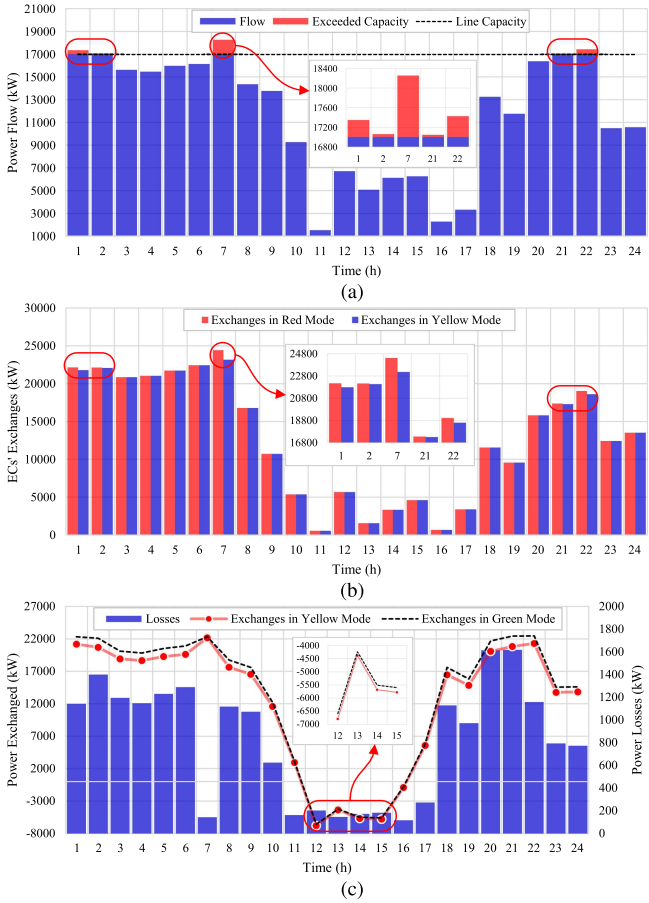

Fig. 7. Analysis of different operation modes. (a) Operation entered red mode. (b) Operation entered yellow mode. (c) Operation entered green mode.

nodes 23, 62, 331, 437, and 476. In contrast, Case 3 shows that the DSO successfully mitigated congestion using downward services provided by ECs.

Fig. 7(a)–(c) depict the performance of the proposed DSO-driven algorithm in red, yellow, and green operating modes. Fig. 7(a) shows the power flow in line 458, indicating congestion during five different hours. Upon detecting congestion, the DSO shifts operations to red mode and sends signals limiting exchanges to the retailer, who then informs EC members and operators of the restrictions. Fig. 7(b) shows the ECs' power exchanges with retailers after applying new restrictions, which reduced coupling point flows, resolved congestion, and triggered yellow mode. In this mode, the DSO computes hourly power losses and notifies the retailer by rerunning the power flow. The retailer then adjusts WSM purchases accordingly. Fig. 7(c) compares the retailer's exchanges before and after receiving loss signals, showing increased WSM purchases to offset losses and maintain balance.

Fig. 8(a) and (b) depict the energy balance and temperatures for an EC member before and after providing grid services. Fig. 8(a) shows that the EC member maintains hot water and room temperatures at residents' preferred levels and charges the EV from 18:00 to 22:00. Fig. 8(b) demonstrates that the member provided downward capacities based on received signals using TCLs, BIS, and V2H systems. As per Fig. 8(b), the

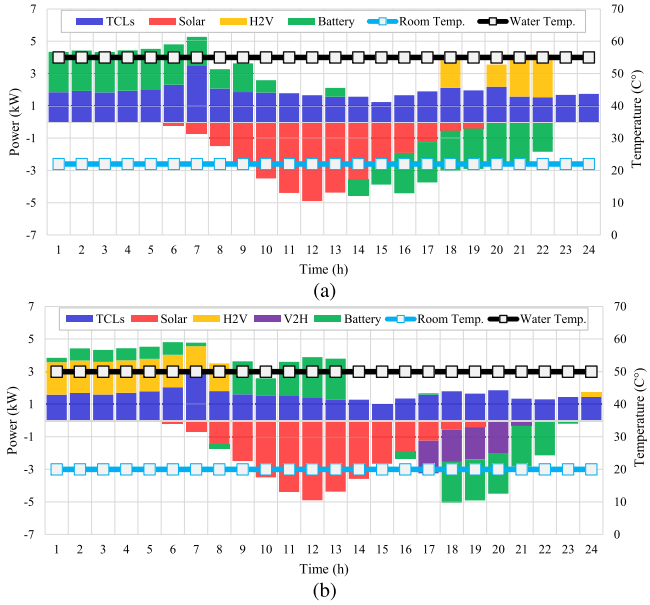

Fig. 8. Schedule obtained for an EC member. (a) Before providing grid services. (b) After providing grid services.

member reduced the operating points of the WH and AC systems throughout the scheduling period, deviating from the preferred water and room temperatures within an acceptable range. In addition, activating V2H allowed the member to discharge both EV and home batteries between 17:00 and 21:00, reducing grid purchases.

VI. Conclusion

This article presents a four-level model for integrating ECs into local electricity markets and maximizing their grid services. It features a decentralized platform for P2P power sharing with dynamic pricing among EC members, and a DSO-driven algorithm for adhering to market exchanges with security constraints while maximizing grid services from local resources. Implemented on a 594-node case study in Victoria, Australia, the results show: 1) Applying the proposed enhanced MMR method on the P2P platform made exchanges on this platform more cost-effective for both buyers and sellers than transactions with upstream agents, lowering their billing costs by 26.59% and 2.5%, respectively. 2) The proposed DSO-driven algorithm enables DSOs to evaluate the feasibility of contracts without accessing their details, communicate corrective signals, and maximize grid services from ECs. 3) This algorithm enabled EC members to plan their BIS, TCLs, and V2H technologies according to the grid services requested by the DSO, reducing their bills by 7.5%. Future research directions include implementing the proposed four-level model on cloud-based platforms to assess its scalability, efficiency, and practical deployment. In addition, evaluating its vulnerability under emergency conditions, such as cyber attacks, will be crucial to enhancing its resilience and security.

References

[1] F. Alfaverh, M. Denai, and Y. Sun, "A dynamic peer-to-peer electricity market model for a community microgrid with price-based demand response," *IEEE Trans. Smart Grid*, vol. 14, no. 5, pp. 3976–3991, Sep. 2023.

[2] H. T. Doan, T. H. B. Huy, D. Kim, and H. Kim, "Fully decentralized peer-to-peer community grid with dynamic and congestion pricing," *IEEE Internet Things J.*, vol. 11, no. 14, pp. 24483–24496, Jul. 2024.

[3] I. F. Reis, I. Gonçalves, M. A. Lopes, and C. H. Antunes, "Towards inclusive community-based energy markets: A multiagent framework," *Appl. Energy*, vol. 307, Feb. 2022, Art. no. 118115.

[4] M. Tostado-Véliz, A. Rezaee Jordehi, D. Icaza, S. A. Mansouri, and F. Jurado, "Optimal participation of prosumers in energy communities through a novel stochastic-robust day-ahead scheduling model," *Int. J. Elect. Power Energy Syst.*, vol. 147, May 2023, Art. no. 108854.

[5] P. Afzali, A. Rajaei, M. Rashidinejad, and H. Farahmand, "Peer-to-peer energy trading among prosumers in energy communities based on preferences considering holacracy structure," *IEEE Trans. Eng. Manag.*, vol. 71, pp. 7756–7767, 2024.

[6] Y. Wu, T. Zhao, H. Yan, M. Liu, and N. Liu, "Hierarchical hybrid multi-agent deep reinforcement learning for peer-to-peer energy trading among multiple heterogeneous microgrids," *IEEE Trans. Smart Grid*, vol. 14, no. 6, pp. 4649–4665, Nov. 2023.

[7] X. Wei, J. Liu, Y. Xu, and H. Sun, "Virtual power plants peer-to-peer energy trading in unbalanced distribution networks: A distributed robust approach against communication failures," *IEEE Trans. Smart Grid*, vol. 15, no. 2, pp. 2017–2029, Mar. 2024.

[8] K. Zhao, M. Zhang, R. Lu, and C. Shen, "A secure intra-regional-inter-regional peer-to-peer electricity trading system for electric vehicles," *IEEE Trans. Veh. Technol.*, vol. 71, no. 12, pp. 12576–12587, Dec. 2022.

[9] H. Ma et al., "Optimal peer-to-peer energy transaction of distributed prosumers in high-penetrated renewable distribution systems," *IEEE Trans. Ind. Appl.*, vol. 60, no. 3, pp. 4622–4632, May/Jun. 2024.

[10] N. Mignoni, R. Carli, and M. Dotoli, "Distributed noncooperative MPC for energy scheduling of charging and trading electric vehicles in energy communities," *IEEE Trans. Control Syst. Technol.*, vol. 31, no. 5, pp. 2159–2172, Sep. 2023.

[11] M. Sivianes, J. M. Maestre, A. Zafra-Cabeza, and C. Bordons, "Blockchain for energy trading in energy communities using stochastic and distributed model predictive control," *IEEE Trans. Control Syst. Technol.*, vol. 31, no. 5, pp. 2132–2145, Sep. 2023.

[12] J. Faraji, F. Vallée, and Z. De Grève, "A preference-informed energy sharing framework for a renewable energy community," *IEEE Trans. Energy Markets, Policy Regulation*, vol. 2, no. 4, pp. 503–518, Dec. 2024.

[13] J. Hong, H. Hui, H. Zhang, N. Dai, and Y. Song, "Distributed control of large-scale inverter air conditioners for providing operating reserve based on consensus with nonlinear protocol," *IEEE Internet Things J.*, vol. 9, no. 17, pp. 15847–15857, Sep. 2022.

[14] H. Hui et al., "A transactive energy framework for inverter-based HVAC loads in a real-time local electricity market considering distributed energy resources," *IEEE Trans. Ind. Informat.*, vol. 18, no. 12, pp. 8409–8421, Dec. 2022.

[15] W. Guedes, C. Oliveira, T. A. Soares, B. H. Dias, and M. Matos, "Collective asset sharing mechanisms for PV and BESS in renewable energy communities," *IEEE Trans. Smart Grid*, vol. 15, no. 1, pp. 607–616, Jan. 2024.

[16] L. He and J. Zhang, "Energy trading in local electricity markets with behind-the-meter solar and energy storage," *IEEE Trans. Energy Markets, Policy Regulation*, vol. 1, no. 2, pp. 107–117, Jun. 2023.

[17] Z.-W. Yu, L. Ding, Z.-M. Kong, Z.-W. Liu, P. Hu, and Y. Xiao, "A distributed coordinated framework with fair comfort level sharing for inverter air conditioner in auxiliary services," *IEEE Trans. Smart Grid*, vol. 15, no. 3, pp. 2776–2790, May 2024.

[18] H. Nagpal, I.-I. Avramidis, F. Capitanescu, and A. G. Madureira, "Local energy communities in service of sustainability and grid flexibility provision: Hierarchical management of shared energy storage," *IEEE Trans. Sustain. Energy*, vol. 13, no. 3, pp. 1523–1535, Jul. 2022.

[19] M. A. Putratama, R. Rigo-Mariani, A. D. Mustika, V. Debusschere, A. Pachurka, and Y. Bésanger, "A three-stage strategy with settlement for an energy community management under grid constraints," *IEEE Trans. Smart Grid*, vol. 14, no. 2, pp. 1505–1514, Mar. 2023.

[20] J. Hong, H. Hui, H. Zhang, N. Dai, and Y. Song, "Event-triggered consensus control of large-scale inverter air conditioners for demand response," *IEEE Trans. Power Syst.*, vol. 37, no. 6, pp. 4954–4957, Nov. 2022.

[21] B.-C. Lai, W.-Y. Chiu, and Y.-P. Tsai, "Multiagent reinforcement learning for community energy management to mitigate peak rebounds under renewable energy uncertainty," *IEEE Trans. Emerg. Topics Comput. Intell.*, vol. 6, no. 3, pp. 568–579, Jun. 2022.

[22] [Online]. Available: https://pascua.iit.comillas.edu/aramos/IData.xlsx